

# Low-coherence interferometric fiber sensor with improved resolution using stepper motor assisted optical ruler

Shih-Hsiang Hsu<sup>a</sup>, Chih-Yuan Tsou<sup>a</sup>, M.-S. Hsieh<sup>b</sup>, Ching-Yu Lin<sup>b,\*</sup>

<sup>a</sup> Department of Electronic Engineering, National Taiwan University of Science and Technology, No. 43, Sec. 4, Keelung Rd., Taipei, Taiwan

<sup>b</sup> School of Medical Laboratory Science and Biotechnology, College of Medical Science and Technology, Taipei Medical University, 250 Wu-Hsing Street, Taipei, Taiwan

## ARTICLE INFO

### Article history:

Received 7 October 2012

Revised 21 January 2013

Available online 6 March 2013

### Keywords:

Interferometer  
Sensor

## ABSTRACT

Low-coherence interferometric sensing is typically used to detect phase changes without simultaneous optical ruler calibration in order to by-pass light intensity fluctuations and the periodic nature of the interferometric signal. An interferogram from a two-staged optical low-coherence Mach–Zehnder interferometer is proposed to double the sensitivity improvement for fiber strain sensing. A 1310-nm wavelength distributed feedback laser implemented in an optical ruler achieved 655-nm resolved characterization from its high-coherence interferogram, which could further be enhanced to an average of 18.9 nm using a stepper motor assisted optical ruler. A 2.7-nε high strain resolution was then demonstrated on a 3-m long fiber sensing arm in a Mach–Zehnder interferometer. The relative movement distances between the interferograms were utilized to experimentally show the strain and force sensitivity as 6.8 μm/με and 8.5 μm/mN, respectively.

© 2013 Elsevier Inc. All rights reserved.

## 1. Introduction

Fiber sensors offer excellent advantages in sensing temperature, concentration, velocity, force, and strain due to their low optical insertion loss, immunity to electromagnetic interference, low cost, light weight, small footprint, and high sensitivity. In the last decade, numerous research accomplishments including the fiber Bragg grating (FBG) [1–3], photonic crystal fiber (PCF) [4,5] and single-mode fiber [6] have advanced fiber strain sensing or fiber force sensing, especially temperature independent multi-sensing [2,4,5] and the spatial division multiplexing system [7,8]. The Fabry–Pérot interferometric (FPI) optical fiber sensor characterized the strain by measuring the cavity length, wavelength shift, and optical path difference [9–12]. Using the optical time domain reflectometry (OTDR) technique, strained polymer optical fibers (POFs) could be tested by evaluating the occurring local Rayleigh backscatter increase [13]. The distributed fiber strain sensor system from the Brillouin optical correlation-domain reflectometry (BOCDR) can sense spatial position and high-speed measurement [14].

The typical sensing approach in the Mach–Zehnder (MZ) interferometer involves directly detecting the output optical power, in which light intensity fluctuation and interferometric signal periods easily produce sensing accuracy. The optical low coherence interferometry (OLCI), one of the most popular sensing technologies,

can be utilized to precisely gauge various physical sensing properties, such as temperature, pressure, force, strain, positioning, vibration, and refractive index using interferograms [15]. The way to solve scanner-induced errors involves monitoring the scanner motion progress and correcting the errors in real time using a closed-loop system [16]. Another simple and economic approach involves improving the spatial resolution using an optical ruler [17]. We propose a stepper motor assisted optical ruler coupled with a two-stage optical low-coherence MZ interferometer using a super-luminescent diode (SLED) for the strain sensing resolution and sensitivity enhancement.

## 2. Design

The majority of fiber interferometric sensors use the first order theory of elasticity and the photoelastic effect in an elastic and mechanically homogeneous fiber. The relationship between phase change  $\Delta\phi$  and elongation  $\Delta L$  is given by the following equation [18]:

$$\begin{aligned} \Delta\phi &= k[n_{\text{fiber}}\Delta L + \Delta n_{\text{fiber}}L] = n_{\text{fiber}}kL\left(\frac{\Delta L}{L} + \frac{\Delta n_{\text{fiber}}}{n_{\text{fiber}}}\right) \\ &= kn_{\text{fiber}}\Delta L\{1 - (n_{\text{fiber}}^2/2)[p_{12} - \nu(p_{11} + p_{12})]\} = kn_{\text{fiber}}\Delta L\xi \quad (1) \end{aligned}$$

where  $L$  is the total fiber length,  $k$  is wave number,  $n_{\text{fiber}}$  is fiber refractive index,  $\Delta n_{\text{fiber}}$  and  $\Delta L$  are variation from fiber refractive index and fiber length difference on MZ interferometer arms, respectively.  $p_{ij}$  is Pockels coefficient, and  $\nu$  is Poisson ratio of the fiber

\* Corresponding author. Fax: +886 2 2737 6424.

E-mail address: PhotonicsNTUST@gmail.com (C.-Y. Lin).

material.  $\xi$  is the strain optic correction factor. Following Eq. (1), the phase detection from the fiber strain variation in the interferometer can be listed as follows:

$$\Delta\phi = (0.79n_{\text{fiber}}\Delta L)k = L_{MD}k \quad (2)$$

In a typical fused-silica fiber,  $\nu = 0.16$ ,  $n_{\text{fiber}} = 1.46$ ,  $p_{11} = 0.113$ ,  $p_{12} = 0.252$ , and  $\xi$  is equal to 0.79, which accounts for the sensitivity reduction due to the stress-optic effect on silica fiber material [18,19].  $L_{MD}$  is the relative movement distance between interferograms and can be demonstrated as the effective length difference between two MZ interferometer arms.

An OLCI system with a low coherence broad light source was used to demonstrate phase-matching using a two-stage optical MZ interferometer, as shown in Fig. 1. The distributed feedback (DFB) laser possessed high coherence length and its interferogram with a 1310-nm wavelength period could be used as an accurate optical ruler. The first MZ interferometer was used for sensing and the second was utilized to analyze the strain effect. The optical path difference between two MZ arms in the first stage was defined as  $\Delta L_1 (=L_a - L_b)$  and the  $\Delta L_2 (=L_c - L_d)$  was movable, representing the phase difference in the second stage.

The output optical intensity from the constant  $\Delta L_1$  and movable collimator position,  $\Delta L_2$ , can be described as follows [7]:

$$I_o \propto 2 \exp\left\{-\frac{1}{2}(k\Delta L_2)^2\right\} + \exp\left\{-\frac{1}{2}[k(\Delta L_2 + \Delta L_1)^2]\right\} + \exp\left\{-\frac{1}{2}[k(\Delta L_2 - \Delta L_1)^2]\right\} \quad (3)$$

The optical intensity relative to the movable collimator positions represented the interferograms for three kinds of optical path differences through two movable collimators, as shown in Fig. 2. We can see that the optical intensity maxima is located at  $\Delta L_2 = 0$ ,  $\Delta L_2 = \Delta L_1$ , and  $\Delta L_2 = -\Delta L_1$  with the high coherence length light source interferogram employing a stable continuous waveform. The sensing arm in the first MZ stage was characterized using different optical collimator movement distance (MD),  $L_{MD}$ , for interferograms. The strain value  $\varepsilon (= \Delta L_1/L)$  of an axially loaded fiber is expressed as the ratio of the sensing length change,  $\Delta L_1$ , to the original fiber length  $L$ . The sensitivity  $S$  in this system can be expressed in the following:

$$L_{MD1} = 0.79n_{\text{fiber}}\Delta L_1 \text{ and } L_{MD2} = 0.79n_{\text{fiber}}(-\Delta L_1) \quad (4)$$

$$S = \frac{L_{MD1} - L_{MD2}}{\varepsilon} = 1.58n_{\text{fiber}}L \quad (5)$$

where the factor 2 comes from the double optical path difference and  $n_{\text{fiber}}$  is the refractive index of a single mode SMF-28 fiber.

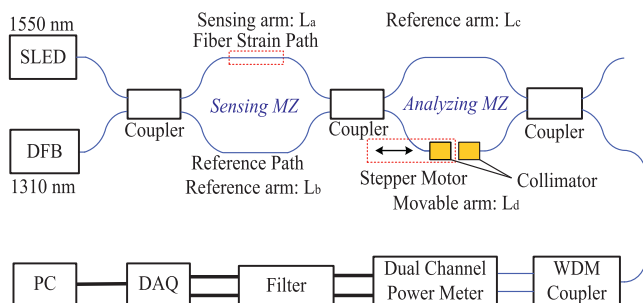


Fig. 1. Two-stage low coherence interferometric fiber strain sensor measurement system.

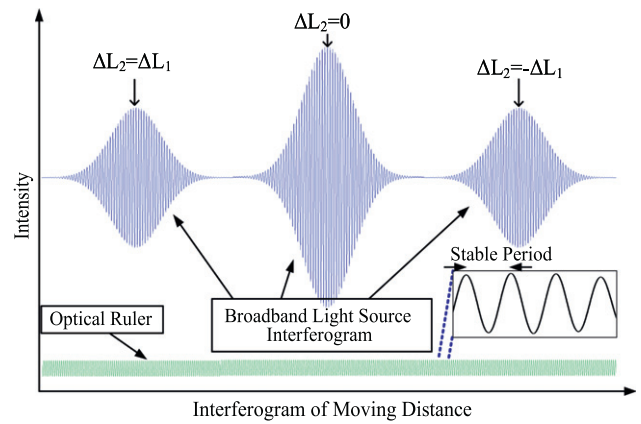


Fig. 2. Optical intensity relative to the movable collimator positions.

### 3. Experiment and discussion

A two-stage OLCI strain measurement system was implemented using the stepper motor demonstrated in Fig. 1. The first optical coupler combined a 57-nm 3 dB spectral width SLED with 1552-nm center wavelength and 1310-nm wavelength DFB laser. Followed by the 2nd optical coupler and sensing arm, the collimators were placed onto a moving platform, located in the 2nd MZ stage and controlled by the stepper motor. A wavelength-division multiplexing (WDM) coupler was used to separate two wavelengths. The optical power was analyzed using a dual channel power meter. The electrical filter and data acquisition (DAQ) card were executed for the noise filtering and analog/digital conversion functions. The relative collimator movement distance represents the interferogram phase difference and can derive the optical path difference in a two-stage MZ interferometer. From Eq. (3), three interferograms are demonstrated using collimator scanning. The three maximum peaks at the phase matching conditions in a two-stage OLCI system are experimentally characterized and demonstrated in Fig. 3. We can therefore gauge the strain from the sensing arm through the double optical path difference by manipulating the distance between the left and right peaks.

This experiment utilized the optical ruler to calibrate the stable stepper motor stage. The collimator movement platform scanning included the stepper motor movement steps on the horizontal axis and DFB laser interferograms in the inset for 1310-nm wavelength stable periods, as shown in Fig. 3. The dual channel optical power meter was used to simultaneously characterize the optical intensity

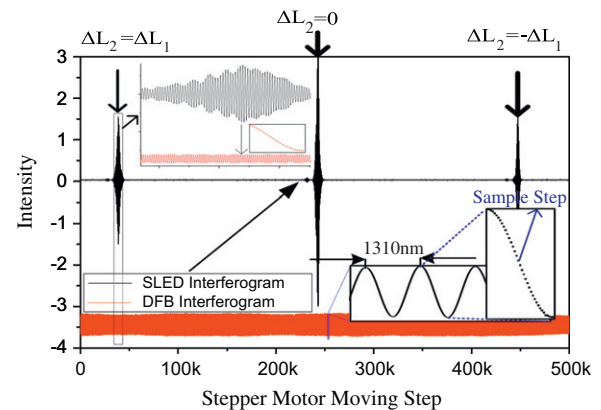


Fig. 3. Optical intensity from movable collimator position.

Download English Version:

<https://daneshyari.com/en/article/10344047>

Download Persian Version:

<https://daneshyari.com/article/10344047>

[Daneshyari.com](https://daneshyari.com)